NUCLEAR SCIENCE AND ENGINEERING: 61, 60-71 (1976)

The Kinetics of a Coupled Two-Core Nuclear Reactor

Felix C. Difilippo* and Ricardo M. Waldman

Comisión Nacional de Energía Atômica, Gerencia de Desarrollo
Departamento de Reactores, Buenos Aires, Argentina

Received September 30, 1975
Revised March 16, 1976

A model is developed to investigate the response of a coupled two-core reactor to a neutron pulse.

Various coupled cores with symmetrical and asymmetrical configurations and compositions are studied. The fundamental spatial mode splits into two distinct decaying submodes. The reactivity of a coupled-core system is defined, and two methods are given for its measurement.

The model is compared with results of pulsed-neutron experiments performed on a light-water-moderated, coupled, compact two-core reactor fueled with uranium of 90% ^{235}U content and reflected by both light water and graphite in either symmetrical or asymmetrical configurations

INTRODUCTION

The pulsed-neutron source method has been extensively utilized in the past to determine both nuclear parameters and reactivities.[1] Recently several improvements in the theoretical formalism as well as in the interpretation of reactivity measurements have been reported by various authors.[2-7]

The interpretation of pulsed source measurements in coupled nuclear systems was initiated by Waltar and Ruby,[8] who described the core reflector interaction by a set of coupling constants and developed a method to measure the reactivity of such a system. Farinelli and Pacilio[9] extended the formalism to the case of two weakly coupled symmetrical cores (i.e., cores with the same fuel and geometry). McDonnell and Harris[10] studied a three-zone coupled system and found difficulties in the interpretation of the experimental results within the framework of their theory.

The purpose of the present work is to correlate pulsed-neutron experimental data with kinetic parameters of coupled-core reactors, for either symmetrical or asymmetrical configurations and compositions.

The model developed here is based on the Cohn[11] formalism under the assumption of two space nodes. It predicts the existence of two submodes exhibiting the same decay constants in both reactor zones. The reactivity for the two-zone system is defined, and an experimental procedure is given that allows the calculation of reactivity on the basis of the measured decay constants.

*Present address: Oak Ridge National Laboratory, Oak Ridge, Tennessee 37830.

[1] *Proc. Symp. Pulsed Neutron Research*, Karlsruhe, Vols. I and II, International Atomic Energy Agency, Vienna (1965).

[2] M. BECKER and K. S. QUISENBERRY, "The Spatial Dependence of Pulsed Neutron Reactivity Measurements," University of Arizona Symp. Neutron Dynamics and Control, University of Arizona (1965).

[3] C. A. PRESKITT, E. A. NEPHEW, J. R. BROWN, and K. R. VAN HOWE, *Nucl. Sci. Eng.*, **29**, 283 (1967).

[4] C. F. MASTERS and K. B. CADY, *Nucl. Sci. Eng.*, **29**, 272 (1967).

[5] T. GOZANI, "Consistent Subcritical Fast Reactor Kinetics," in *Dynamics of Nuclear Systems*, p. 109, University of Arizona Press, Tucson, Arizona (1972).

[6] F. C. DIFILIPPO, N. B. PIERONI, and J. C. VIÑEZ, *Nucl. Sci. Eng.*, **51**, 262 (1973).

[7] G. KOSALY et al., *Atomkernenergie*, **23**, 251 (1974).

[8] A. WALTAR and L. RUBY, *Nukleonik*, **8**, 287 (1966).

[9] U. FARINELLI and N. PACILIO, *Nucl. Sci. Eng.*, **36**, 39 (1969).

[10] F. N. McDONNELL and M. HARRIS, *J. Nucl. Energy*, **26**, 129 (1972).

[11] C. E. COHN, *Nucl. Sci. Eng.*, **13**, 12 (1962).

THEORY

Reactor Response to a Periodic Rectangular Neutron Source

The Cohn formalism sets the hypothesis that the reactor can be spatially divided in regions and that each region can be characterized by global kinetic parameters. The boundary conditions between regions appear through coupling coefficients.

For the particular case of two coupled cores, the equations are:

$$\frac{dN_1(t)}{dt} = \alpha_1 N_1(t) + \Lambda_{21} N_2(t) + \sum_{i=1}^{m_1} \lambda_{1i} C_{1i}(t) + J \sum_{n=0}^{L-1} [H(t - nT) - H(t - nT - d)] \quad (1)$$

$$\frac{dN_2(t)}{dt} = \alpha_2 N_2(t) + \Lambda_{12} N_1(t) + \sum_{r=1}^{m_2} \lambda_{2r} C_{2r}(t) \quad (2)$$

$$\frac{dC_{1i}(t)}{dt} = -\lambda_{1i} C_{1i}(t) + \Gamma_{1i} N_1(t) \quad (3)$$

$$\frac{dC_{2r}(t)}{dt} = -\lambda_{2r} C_{2r}(t) + \Gamma_{2r} N_2(t) \quad , \quad (4)$$

where

$N_i(t)$ = total number of neutrons in region i, at time t

$\alpha_i = \dfrac{K_i(1 - \beta_i) - 1}{l_i}$ = time constant for the i'th region

K_i = probability that a neutron removed in region i will produce a fission neutron in the same region

l_i = mean life of neutrons in region i

$\Lambda_{ij} = K_{i \to j}/l_i$

$K_{i \to j}$ = probability that a neutron removed from region i will contribute to the neutron population in region j

$C_{ij}(t)$ = total number of type j delayed neutron precursors in region i at time t

m_i = total number of delayed neutron precursor groups in region i

λ_{ij} = decay constants of precursor j in region i

$H(t - \tau)$ = step function

J = source intensity

L = total number of pulses emitted by the source

T = inverse pulse rate (sec)

d = pulsed-neutron width

$\Gamma_{ij} = \beta_{ij} K_i/l_i$

β_{ij} = delayed neutron fraction of precursor j in region i

$\beta_i = \sum_{j=1}^{m_i} \beta_{ij}$, total delayed neutron fraction in region i

On application of the Laplace transform to Eqs. (1) through (4), we obtain for the transformed neutron population:

$$n_1(s) = \frac{J\left[(s - \alpha_2)\prod_{r=1}^{m_2}(s + \lambda_{2r}) - \sum_{r=1}^{m_2}\lambda_{2r}\Gamma_{2r}\prod_{\substack{\mu=1 \\ \mu \neq r}}^{m_2}(s + \lambda_{2\mu})\right]\prod_{i=1}^{m_1}(s + \lambda_{1i})\left\{\sum_{n=0}^{L-1}\frac{\exp(-nTs)}{s}[1 - \exp(-ds)]\right\}}{\prod_{k=1}^{m_1+m_2+2}(s - \gamma_k)} \quad (5)$$

$$n_2(s) = \frac{J\,\Lambda_{12}\prod_{i=1}^{m_1}(s + \lambda_{1i})\prod_{r=1}^{m_2}(s + \lambda_{2r})\sum_{n=0}^{L-1}\frac{\exp(-nTs)}{s}[1 - \exp(-ds)]}{\prod_{k=1}^{m_1+m_2+2}(s - \gamma_k)} \quad , \quad (6)$$

where

$$\prod_{k=1}^{m_1+m_2+2}(s-\gamma_k) = (s-\alpha_1)(s-\alpha_2)\prod_{i=1}^{m_1}(s+\lambda_{1i})\prod_{r=1}^{m_2}(s+\lambda_{2r}) - \left[(s-\alpha_1)\prod_{i=1}^{m_1}(s+\lambda_{1i})\sum_{r=1}^{m_2}\lambda_{2r}\Gamma_{2r}\prod_{\substack{\mu=1\\ \mu\neq r}}^{m_2}(s+\lambda_{2\mu})\right.$$
$$\left. + (s-\alpha_2)\prod_{r=1}^{m_2}(s+\lambda_{2r})\sum_{i=1}^{m_1}\lambda_{1i}\Gamma_{1i}\prod_{\substack{j=1\\ j\neq i}}^{m_1}(s+\lambda_{1j})\right] + \left[\sum_{i=1}^{m_1}\lambda_{1i}\Gamma_{1i}\prod_{\substack{j=1\\ j\neq i}}^{m_1}(s+\lambda_{1j})\right]$$
$$\times\left[\sum_{r=1}^{m_2}\lambda_{2r}\Gamma_{2r}\prod_{\substack{\mu=1\\ \mu\neq r}}^{m_2}(s+\lambda_{2\mu})\right] - \Lambda_{12}\Lambda_{21}\prod_{i=1}^{m_1}(s+\lambda_{1i})\prod_{r=1}^{m_2}(s+\lambda_{2r}) \quad . \tag{7}$$

Laplace inversion of the resulting equations and utilization of the multichannel time, Θ (related with t by $t = nT + \Theta$, $0 \leq n \leq L-1$, $0 \leq \Theta \leq T$), yield the following results, after adding the contribution from each pulse:

$$N_1(\Theta) = J\sum_{k=1}^{m_1+m_2+2}\frac{(\gamma_k-\alpha_2)\prod_{r=1}^{m_2}(\gamma_k+\lambda_{2r})\prod_{i=1}^{m_1}(\gamma_k+\lambda_{1i})}{\gamma_k\sum_{\substack{l=1\\ l\neq k}}^{m_1+m_2+2}(\gamma_k-\gamma_l)}\left\{\left[\frac{1}{1-\exp(-\gamma_k T)}+\frac{1-\exp(\gamma_k LT)}{2-\exp(-\gamma_k T)-\exp(\gamma_k T)}\right]\right.$$
$$\left.\times[1-\exp(-\gamma_k d)]\right\}\exp(\gamma_k\Theta) \tag{8}$$

$$N_2(\Theta) = J\sum_{k=1}^{m_1+m_2+2}\Lambda_{12}\frac{\prod_{i=1}^{m_1}(\gamma_k+\lambda_{1i})\prod_{r=1}^{m_2}(\gamma_k+\lambda_{2r})}{\gamma_k\sum_{\substack{l=1\\ l\neq k}}^{m_1+m_2+2}(\gamma_k-\gamma_l)}\left\{\left[\frac{1}{1-\exp(-\gamma_k T)}+\frac{1-\exp(\gamma_k LT)}{2-\exp(-\gamma_k T)-\exp(\gamma_k T)}\right]\right.$$
$$\left.\times[1-\exp(-\gamma_k d)]\right\}\exp(\gamma_k\Theta) \tag{9}$$

for the case $d \leq \Theta \leq T$.

On the basis of arguments similar to the ones of Waltar and Ruby,[12] it can be shown that two of the $(m_1 + m_2 + 2)$ roots, which we call γ_1 and γ_2, correspond to the prompt-neutron decaying population, where γ_1 is the coupling submode and γ_2 is the persistent one. The other $(m_1 + m_2)$ roots correspond to the decay of the delayed neutron population.

With a proper choice of the pulse rate, one achieves the equilibrium pulse condition, described by Eq. (10) below:

$$\frac{1}{|\gamma_1|} < \frac{1}{|\gamma_2|} \ll T;\ \frac{1}{|\gamma_i|} \gg T\ (i = 3, 4, \ldots, m_1+m_2+2);\ |\gamma_j LT| \gg 1\ (j = 1, 2, \ldots, m_1+m_2+2)\ . \tag{10}$$

In this case, Eqs. (8) and (9) reduce to:

$$N_1(\Theta) = Jd[\bar{A}_1\exp(\gamma_1\Theta) + \bar{B}_1\exp(\gamma_2\Theta) + C_1] \tag{11}$$

$$N_2(\Theta) = Jd[\bar{A}_2\exp(\gamma_1\Theta) + \bar{B}_2\exp(\gamma_2\Theta) + C_2]\ , \tag{12}$$

where

$$\bar{A}_i = \frac{A_i}{d}\frac{1-\exp(-\gamma_1 d)}{\gamma_1} \quad (i = 1, 2) \tag{13}$$

$$\bar{B}_i = \frac{B_i}{d}\frac{1-\exp(-\gamma_2 d)}{\gamma_2} \quad (i = 1, 2) \tag{14}$$

$$A_1 = \frac{(\gamma_1-\alpha_2)\prod_{i=1}^{m_1}(\gamma_1+\lambda_{1i})\prod_{r=1}^{m_2}(\gamma_1+\lambda_{2r})}{\prod_{l=2}^{m_1+m_2+2}(\gamma_1-\gamma_l)} \cong \frac{\gamma_1-\alpha_2}{\gamma_1-\gamma_2} \tag{15}$$

[12] A. WALTAR and L. RUBY, *Nukleonik*, **10**, 70 (1967).

$$B_1 = \frac{(\gamma_2 - \alpha_2)\prod_{i=1}^{m_1}(\gamma_2 + \lambda_{1i})\prod_{r=1}^{m_2}(\gamma_2 + \lambda_{2r})}{\prod_{\substack{l=1 \\ l\neq 2}}^{m_1+m_2+2}(\gamma_2 - \gamma_l)} \cong \frac{\gamma_2 - \alpha_2}{\gamma_2 - \gamma_1} \tag{16}$$

$$C_1 = \sum_{k=3}^{m_1+m_2+2}(\gamma_k - \alpha_2)\frac{\prod_{i=1}^{m_1}(\gamma_k + \lambda_{1i})\prod_{r=1}^{m_2}(\gamma_k + \lambda_{2r})}{\prod_{\substack{l=1 \\ l\neq k}}^{m_1+m_2+2}(\gamma_k - \gamma_l)}\left[\frac{1 + \left(\frac{\Theta}{T} - \frac{1}{2}\right)\gamma_k T}{\gamma_k T}\right]$$

$$\cong \sum_{k=3}^{m_1+m_2+2}\frac{(\gamma_k - \alpha_2)\prod_{i=1}^{m_1}(\gamma_k + \lambda_{1i})\prod_{r=1}^{m_2}(\gamma_k + \lambda_{2r})}{T\gamma_k \prod_{\substack{l=1 \\ l\neq k}}^{m_1+m_2+2}(\gamma_k - \gamma_l)} \tag{17}$$

$$A_2 = \frac{\Lambda_{12}\prod_{i=1}^{m_1}(\gamma_1 + \lambda_{1i})\prod_{r=1}^{m_2}(\gamma_1 + \lambda_{2r})}{\prod_{l=2}^{m_1+m_2+2}(\gamma_1 - \gamma_l)} \cong \frac{\Lambda_{12}}{\gamma_1 - \gamma_2} \tag{18}$$

$$B_2 = \frac{\Lambda_{12}\prod_{i=1}^{m_1}(\gamma_1 + \lambda_{1i})\prod_{r=1}^{m_2}(\gamma_1 + \lambda_{2r})}{\prod_{\substack{l=1 \\ l\neq 2}}^{m_1+m_2+2}(\gamma_2 - \gamma_l)} \cong \frac{\Lambda_{12}}{\gamma_2 - \gamma_1} \tag{19}$$

$$C_2 = \sum_{k=3}^{m_1+m_2+2}\Lambda_{12}\frac{\prod_{i=1}^{m_1}(\gamma_k + \lambda_{1i})\prod_{r=1}^{m_2}(\gamma_k + \lambda_{2r})}{\prod_{\substack{l=1 \\ l\neq k}}^{m_1+m_2+2}(\gamma_k - \gamma_l)}\left[\frac{1 + \left(\frac{\Theta}{T} - \frac{1}{2}\right)\gamma_k T}{\gamma_k T}\right]$$

$$\cong \sum_{k=3}^{m_1+m_2+2}\Lambda_{12}\frac{\prod_{i=1}^{m_1}(\gamma_k + \lambda_{1i})\prod_{r=1}^{m_2}(\gamma_k + \lambda_{2r})}{T\gamma_k \prod_{\substack{l=1 \\ l\neq k}}^{m_1+m_2+2}(\gamma_k - \gamma_l)} \quad . \tag{20}$$

Equations (11) and (12) show that the decay constants are global parameters, identical in both regions. Then, in principle, a least-squares fit of the experimental data to a double exponential yields the values of γ_1 and γ_2 as well as the relative amplitudes A_i, B_i, and C_i, apart from a common multiplicative constant.

Derivation and Properties of the Prompt-Neutron Decay Constants

Approximate expressions for γ_1 and γ_2 can be obtained from Eq. (7) by neglecting all terms of degree $<(m_1 + m_2)$ in s. In this way one obtains a quadratic equation with the two roots

$$\gamma_{1,2} = \frac{\alpha_1 + \alpha_2}{2} \mp \left[\left(\frac{\alpha_2 - \alpha_1}{2}\right)^2 + \Lambda_{12}\Lambda_{21}\right]^{1/2} \quad . \tag{21}$$

This procedure is justified by order of magnitude arguments. It can be verified that all the coefficients of the terms of degree $<(m_1 + m_2)$, in s are multiple combinations of λ_{ij} and can be neglected in comparison with the higher degree terms.

Next, in view of the properties of quadratic equations, one obtains the relations

$$\gamma_1 + \gamma_2 = \alpha_1 + \alpha_2 \tag{22}$$

$$\gamma_1 \gamma_2 = \alpha_1\alpha_2 - \Lambda_{12}\Lambda_{21} \quad , \tag{23}$$

and from Eq. (21) we have

$$|\gamma_1| - |\gamma_2| = 2\left[\left(\frac{\alpha_2 - \alpha_1}{2}\right)^2 + \Lambda_{12}\Lambda_{21}\right]^{1/2} \quad . \tag{24}$$

Equations (22), (23), and (24) relate observable quantities (γ_1 and γ_2) with kinetic parameters.

The following limiting cases are of interest: (a) no coupling ($\Lambda_{12} = \Lambda_{21} = 0$) and (b) strong coupling. For the former case we obtain from the respective equations the relations

$$\gamma_1 = \alpha_2;\ \gamma_2 = \alpha_1;\ \bar{A}_1 = \bar{A}_2 = \bar{B}_2 = C_2 = 0 \quad .$$

Physically, it means that in the sourceless core, the neutron population vanishes because of the zero coupling condition. In the core with the source, there is only one decay constant, as is predicted by point kinetic theory.

For strong coupling the γ_1 root is very large and, for all practical purposes, the temporal behavior of the system is controlled by the γ_2 root in agreement with the expected one-point reactor kinetics results.

From Eq. (21), it is indicated that the γ_1 root is never zero; conversely, γ_2 is zero for the prompt critical condition

$$\frac{K_1 + K_2 + K - K_1K_2 - 1}{\beta_1K_1(1 - K_2) + \beta_2K_2(1 - K_1) + \beta_1\beta_2K_1K_2} = 1 \quad , \tag{25}$$

where

$$K = K_{1\to 2}K_{2\to 1} \quad . \tag{26}$$

Reactivity in Dollar Units

Any suitable definition of the concept of global reactivity for a coupled system must conform with the condition of zero value for a critical system and unity for the prompt-critical condition. These restrictions are fulfilled by the definition, Eq. (27), below, where the symbol, \$, represents the reactivity in "dollars," and the subscript refers to the coupled cores:

$$\$_{ac} = \frac{K_1 + K_2 + K - K_1K_2 - 1}{\beta_1K_1(1 - K_2) + \beta_2K_2(1 - K_1) + \beta_1\beta_2K_1K_2} \quad . \tag{27}$$

This is easily verified to be the case because, from the criticality condition,

$$K_1 + K_2 + K - K_1K_2 - 1 = 0 \quad , \tag{28}$$

obtained from Eqs. (1) through (4), Eq. (27) gives zero for the reactivity.

For the prompt critical condition, Eq. (27) yields unity for the reactivity, as can be seen by Eqs. (25) and (27).

This definition of global reactivity is more general than the one used by Farinelli and Pacilio,[9] since ours also applies for asymmetrical coupled reactors and the case of the two coupled cores with different compositions.

Determination of the Global Reactivity

Here we propose two methods to obtain the reactivity of the system.

Reactivity Determination from Coupled Reactor Data

Equation (23) can be written as

$$\gamma_1\gamma_2 = \frac{\beta_1K_1(1 - K_2) + \beta_2K_2(1 - K_1) + \beta_1\beta_2K_1K_2 + (1 + K_1K_2 - K_1 - K_2 - K)}{l_1l_2} \quad , \tag{29}$$

which reduces to the following in the critical case:

$$(\gamma_1\gamma_2)_c = \left[\frac{\beta_1K_1(1 - K_2) + \beta_2K_2(1 - K_1) + \beta_1\beta_2K_1K_2}{l_1l_2}\right] \quad . \tag{30}$$

Under the assumption that the right side of Eq. (30) is a slowly changing function of reactivity, from the two last equations and the definition of reactivity one obtains

$$\$_{ac} = 1 - \frac{\gamma_1\gamma_2}{(\gamma_1\gamma_2)_c} \quad . \tag{31}$$

This result can be interpreted as a generalization of the Simmons and King[13] method. Hence, under the assumption of small reactivity changes, the reactivity of the assembly can be obtained from two measurements of the decay constants for the critical and subcritical conditions.

Reactivity Determination by Sequential Measurements in Isolated Reactor Zones

If we consider the isolated cores, i ($i = 1, 2$), the reactivity in dollar units is, by definition,

$$\$_i = \frac{K_i - 1}{\beta_iK_i} \quad , \tag{32}$$

[13] B. E. SIMMONS and J. S. KING, *Nucl. Sci. Eng.*, **3**, 515 (1958).

which can be related to the prompt decay constant, α_i, through the Inhour equation

$$\$_i = 1 - \frac{\alpha_i}{\alpha_{gi}} \; ; \quad \alpha_{gi} = \frac{K_i \beta_i}{l_i} \quad . \tag{33}$$

From these last two equations we obtain

$$K_i = \frac{1}{\$_i \beta_i - 1} \tag{34}$$

$$l_i = \frac{1 - \$_i}{\alpha_i} \frac{\beta}{1 - \beta_i \$_i} \quad . \tag{35}$$

For weak coupling, one can neglect the changes in K_i and l_i, when the cores are coupled.

Solving for K from Eq. (24) and utilizing Eqs. (34) and (35) yields

$$K = \frac{(1 - \$_1)(1 - \$_2)\beta_1\beta_2}{4\alpha_1\alpha_2(1 - \beta_1\$_1)(1 - \beta_2\$_2)} [(\gamma_1 - \gamma_2)^2 - (\alpha_1 - \alpha_2)^2] \; , \tag{36}$$

and from Eqs. (27), (34), and (36)

$$\$_{ac} = \frac{4\alpha_1\alpha_2\$_1\$_2 - (1 - \$_1)(1 - \$_2)[(\gamma_1 - \gamma_2)^2 - (\alpha_1 - \alpha_2)^2]}{4\alpha_1\alpha_2(1 - \$_1 - \$_2)} \quad . \tag{37}$$

The result, Eq. (37), shows that one can determine the reactivity of the weak coupled reactor by measurements of the reactivities and decay constants in each reactor zone. This reactivity determination, contrary to the previous method, d_1, is also valid for large reactivities.

Limiting Cases

It can be verified directly that if the coupled reactor is symmetric, $K_1 = K_2$, $\beta_1 = \beta_2$, $l_1 = l_2$, the formalism, except the reactivity, is reduced to that of Farinelli and Pacilio.[9]

If one of the regions is a reflector, $K_2 = \beta_2 = 0$, the model coincides with that of Waltar and Ruby.[12]

EXPERIMENTAL SETUP

Multiplying System

Measurements were performed at the critical facility, RA-2, which is a swimming pool experimental reactor. A schematic drawing of this system is shown in Fig. 1.

The standard fuel elements contained 19 Materials Testing Reactor (MTR)-type plates, with

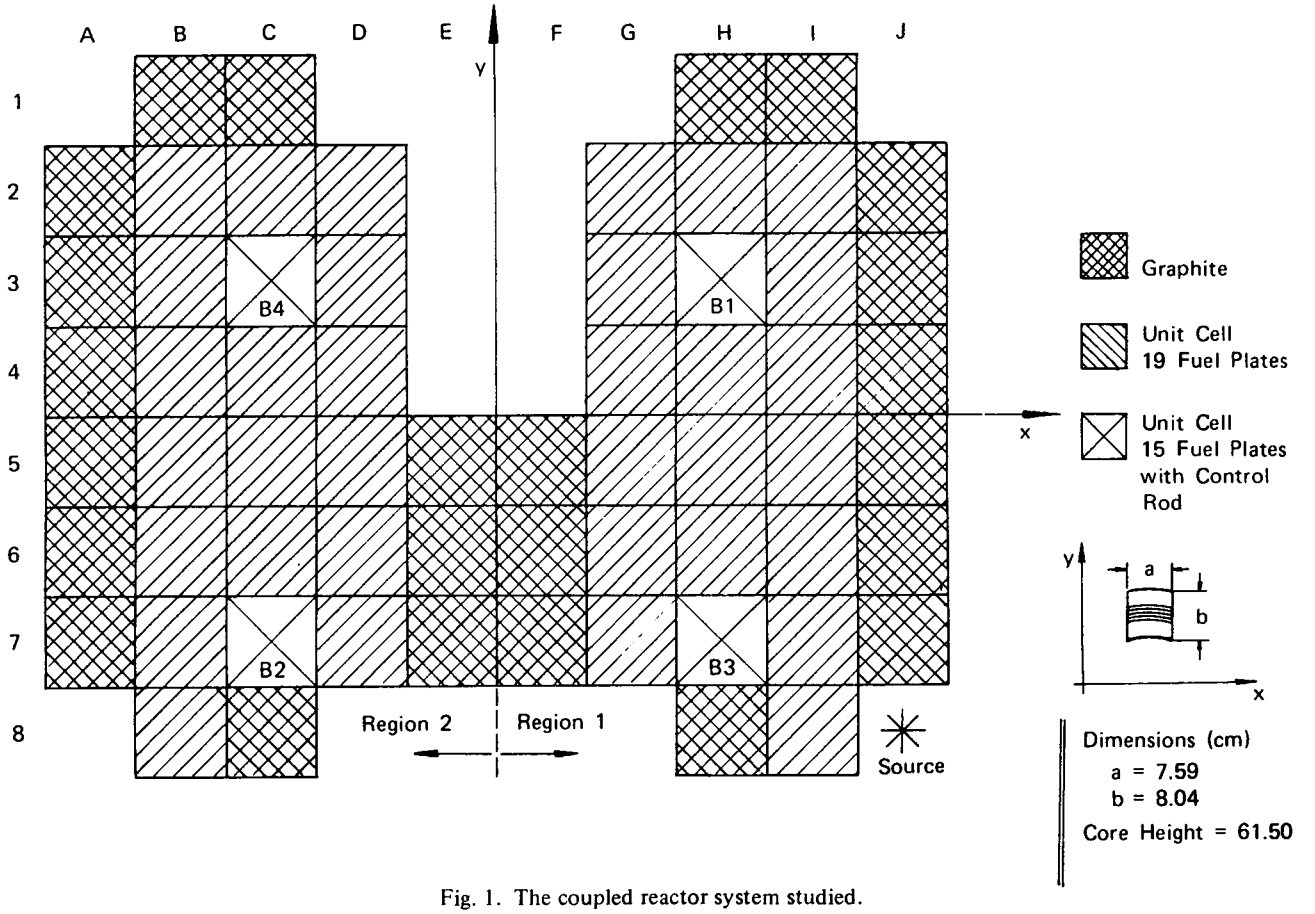

Fig. 1. The coupled reactor system studied.

each aluminium-clad plate containing 8.53 g of 90%-^{235}U-enriched uranium. The elements that contain safety rods had 15 plates. In some of the fuel elements, two special plates were used to allow the insertion of a neutron detector. The graphite elements were also clad in aluminium, except one, which was specially constructed to place the detector inside it. This graphite element was placed in the F-5 position of the assembly during the measurements in the cores. For the reflector-region measurements, the special graphite element was used in each measuring location. The presence of this graphite element introduced a slight asymmetry.

The reference coupled-core reactor was critical with all control rods withdrawn. The different configurations were obtained by the insertion of control rods to minimize the changes of coupling between zones.

Detection System

The detection system utilized was a ^{3}He detector Reuter-Stokes model SK586, 6 mm in diameter, with an active length of 10 cm. A preamplifier, ORTEC Model 109 PC, and an amplifier, ORTEC Model 410 fed a multichannel analyzer, Hewlett-Packard model 5401B, interfaced with an H.P. 9820A computer. The data from the multichannel and computer were transferred to the cassette memory H.P. 9865A.

Pulsed Source

The pulsed-neutron source was a Phillips generator (Model 18600R), polarized and modulated by the same BS2 system. The source was in the J-8 position along the horizontal plane of symmetry, hence, only even harmonics were excited in the z axis. The source position along the x axis was chosen so that the source neutrons would have the maximum probability for a first collision in reactor region 1 (see Fig. 1 for details). This was necessary to implement the assumptions involved in the theoretical model. Due to space limitations in the reactor grid, the y coordinate of the source position could not be optimized from the point of view of the excitation of the higher harmonics of the neutron flux.

Figure 2 shows a block diagram of the electronics and data processing system.

EXPERIMENTAL PROCEDURE

The neutron detector was moved along the x axis at a constant position in the y-z plane

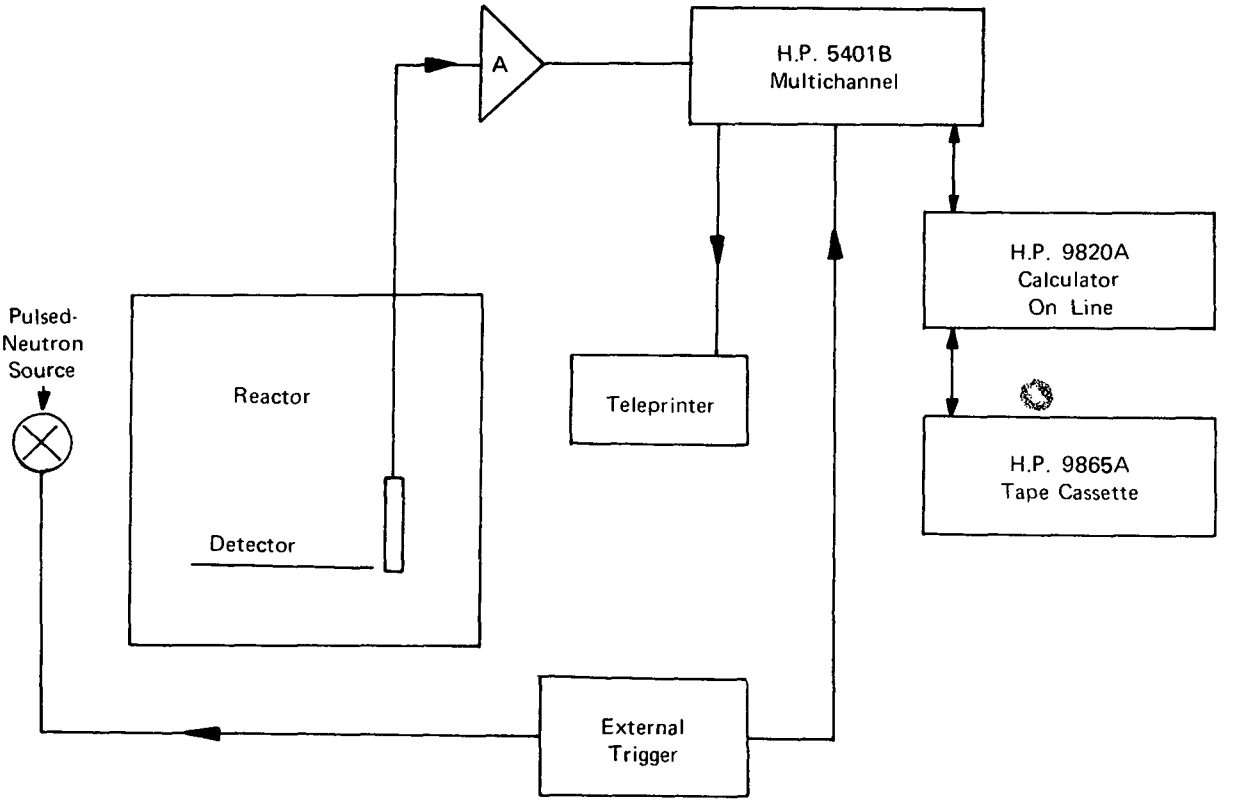

Fig. 2. Detecting and processing system.

corresponding to zero of the first even-source mode.

The measurement of the decay constants at criticality is relatively difficult because of the low signal-to-background ratio. For this reason each measurement was repeated several times to improve the statistical accuracy.

For the subcritical measurements, the background noise was measured before starting the neutron source. Afterward, the source was operated for 3 min so that one reaches an asymptotic delayed neutron population. Then the actual counting occurs to a desired statistical accuracy (~ 60 000 counts at the peak of the pulse).

The neutron pulse width was 800 μsec, and the pulse repetition rate was kept constant for each set of measurements.

A variable channel width was selected to optimize the unfolding of the two exponential contributions to the prompt tail of the pulse.

Previously we have shown, in Eqs. (11) and (12), that the response of the coupled reactor to a neutron pulse train is

$$N_i(\Theta) = Jd[\bar{A}_i \exp(\gamma_1\Theta) + \bar{B}_i \exp(\gamma_2\Theta) + C_i] \quad (i = 1, 2) \quad .$$

The fit of experimental data to the above equation was performed utilizing a nonlinear least-squares-fit program[14] for the on-line computer, after proper corrections were made for dead-time losses and noise background.

More detailed calculations were done with the off-line IBM-370 computer to study the effect of higher harmonics by changing the starting channel in each successive calculation.[15]

The statistical errors of the fitted parameters were determined following the procedure discussed by Orear,[16] who made the hypothesis of a Gaussian distribution in the number of counts. The isolated region, for each rod position, was implemented by removing the other region. As a result, enough grid positions were available to locate the source so that one could minimize the excitation of higher space harmonics. The decay constants in the isolated-region experiment were obtained by a least-squares fit of the prompt tail of the neutron pulse.

The reactivity of the isolated regions were measured according to the method of Gozani,[17] of Garelis and Russell,[18] and of Sjostrand.[19] The analysis was performed with a version of the Trifido[20] program for the on-line computer. In this measurement, the detector was located inside the core to avoid kinetic distortion.[6] In all cases good agreement between the methods of Gozani and Garelis and Russell was obtained, and the reactivity was taken to be the average of those obtained from the two methods.

In the fitting procedure, the parameters were selected according to a χ^2 test and their consistency as a function of the starting channel in the fit.

CORRECTIONS AND EXPERIMENTAL ERRORS

The values of the measured amplitudes have to be corrected for finite channel width. To implement this correction, to each channel we associate a characteristic time at the center of the channel. For an exponential decay, $\bar{A}_i \exp(\gamma_1\Theta)$, the measured count rate is

$$\bar{N}_i \exp(\Theta) = \frac{1}{\Delta t}\int_{\theta-\Delta t/2}^{\theta+\Delta t/2} \bar{A}_i \exp(\gamma_1\Theta)\,d\Theta = \frac{\bar{A}_i}{\gamma_1\Delta t}\frac{1 - \exp(-\gamma_1\Delta t)}{\exp(-\gamma_1\Delta t/2)}\exp(\gamma_1\Theta) \quad ,$$

with a similar expression for the other exponential terms. Then, taking into account Eqs. (13) and (14), the following relations between the measured amplitudes and A_i, B_i are obtained:

$$A_i = \bar{A}_i^{\exp}\frac{\gamma_1^2 d\,\Delta t \exp(-\gamma_1\Delta t/2)}{[1 - \exp(-\gamma_1\Delta t)][1 - \exp(-\gamma_1 d)]} \quad (38)$$

$$B_i = \bar{B}_i^{\exp}\frac{\gamma_2^2 d\,\Delta t \exp(-\gamma_2\Delta t/2)}{[1 - \exp(-\gamma_2\Delta t)][1 - \exp(-\gamma_2 d)]} \quad . \quad (39)$$

The decay constants were corrected by the perturbation produced by the special plates and the detector. In the coupled system the perturbation was measured by the period method, and it amounted to 7 cents of reactivity. For the isolated cores the reactivity perturbation was larger by a factor of 2.3 (see Table I).

[14]F. C. DIFILIPPO and R. M. WALDMAN, "The Model 20 in Reactor Physics," submitted to *Keyboard*, a publication of Hewlett-Packard.

[15]F. C. DIFILIPPO and R. M. WALDMAN, "Método de Ajuste por Cuadrados Mínimos de Funciones no Lineales. Un caso Particular: el Código WARU I.," CNEA Re-88, Comisión Nacional de Energía Atómica (1974).

[16]J. OREAR, "Notes on Statistics for Physicists," UCRL-8417, Lawrence Radiation Laboratory, Berkeley, California (1958).

[17]T. GOZANI, *Nukleonik*, **4**, 348 (1962).

[18]E. GARELIS and J. L. RUSSELL, *Nucl. Sci. Eng.*, **29**, 283 (1963).

[19]N. G. SJOSTRAND, *Ark. Fys.*, **11**, 233 (1956).

[20]F. C. DIFILIPPO and N. B. PIERONI, *Nucl. Sci. Eng.*, **46**, 166 (1971).

TABLE I

Reactivity of Rod B_3 in the Coupled Reactor ($\$_{ac}$) Using Eq. (37), and in the Isolated Core ($\$_1$) Using the Average Between the Gozani and Garelis and Russell Methods

B_3% ↑	$\$_{ac}$	$\$_1$	$\$_1/\$_{ac}$
75	0.235 ± 0.05	0.54 ± 0.05	2.4 ± 0.6
50	0.810 ± 0.08	1.86 ± 0.05	2.3 ± 0.2
25	1.48 ± 0.12	3.57 ± 0.06	2.4 ± 0.2
0	1.90 ± 0.21	4.25 ± 0.07	2.25 ± 0.25

RESULTS AND INTERPRETATION

A typical response of the detector in core 1 can be seen in Fig. 3. The various measurements allowed testing the following aspects of the model:

1. The decay constants are independent of the measuring point. The modal amplitudes exhibited some spatial dependence. Figure 4 shows that the values obtained for γ_1 and γ_2, as a function of the measuring point, are essentially constant as predicted by the model. The observed slight spatial dependence of the decay constants, γ_1 and γ_2, in

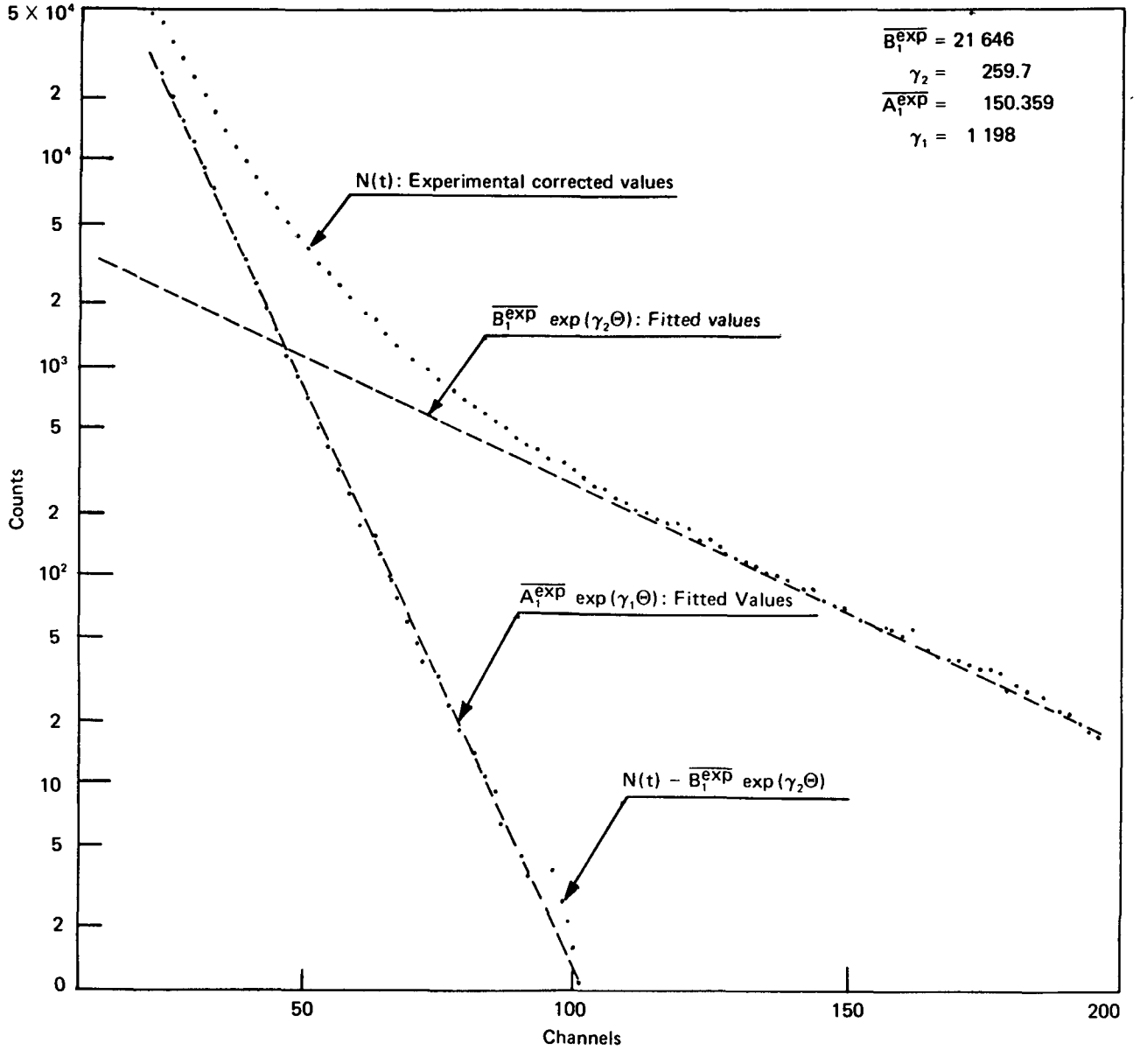

Fig. 3. Equilibrium pulse with the detector and source in region 1.

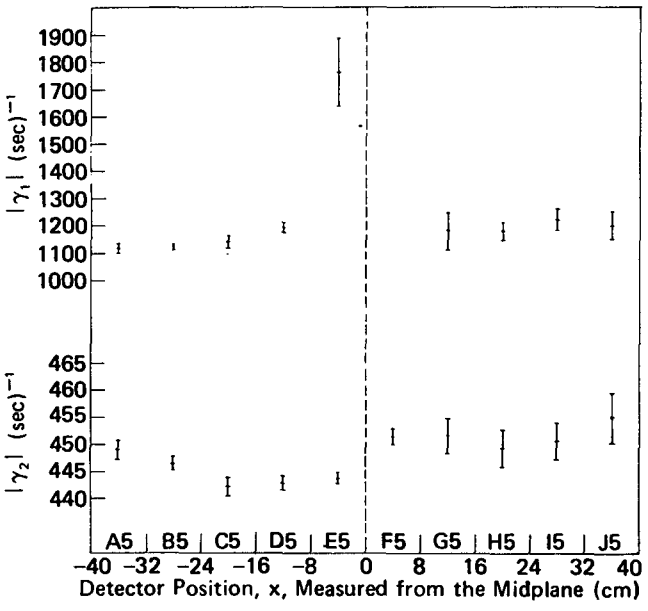

Fig. 4. The terms γ_1 and γ_2 as functions of detector position.

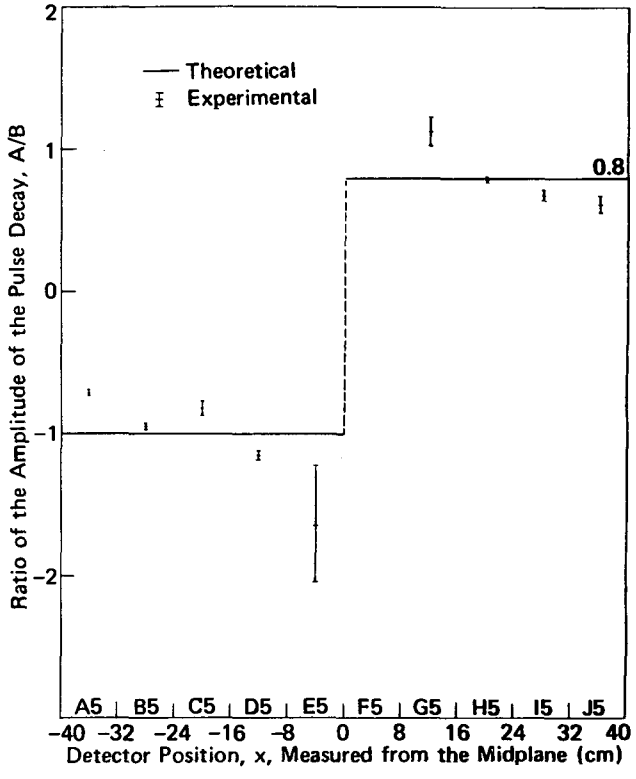

Fig. 5. The term A/B as a function of detector position.

the two regions is consistent with the presence of some harmonic contamination due to the highly asymmetric location of the source.

The values shown in Fig. 4 correspond to the control rod configurations, B_2, B_3 0%↑, B_1, B_4 100%↑ (%↑ means the percent of the rod withdrawn). There is, however, a sharp variation of γ_1 near the central location. This is due to the well-known fact[12] that in this region the γ_1 submode has a very low amplitude due to destructive interference between the signals coming from the two regions. Figure 5 shows (for the same configuration) a comparison of the experimentally obtained A/B ratios with the theoretical values computed according to Eqs. (15), (16), (18), and (19), where the measured values of the various decay constants were utilized as input parameters. Generally good agreement was found between theory and experiment. The observed deviations of the experimental point from the theoretical behavior reflect the fact that the two-node model does not take into account the spatial dependence within each node. The value of the A/B ratio for the region that contains the neutron source is very sensitive to the degree of symmetry between the two cores. This can be seen in Fig. 5, where the small asymmetry produced by the special graphite element makes the value of the A/B ratio drop from unity to 0.8.

This fact is further emphasized later in Table V where variations as large as a factor of 30 can be observed as a function of control rod position in the core. This change is much larger than the variations observed in the decay constants, γ_1 and γ_2.

2. For weak coupling, the time constants, α_1 and α_2, will be nearly equal to the decay constants observable in each of the isolated cores. This fact provides a check of the model through Eq. (22). Tables II and III show the generally, good agreement found for both symmetrical and asymmetrical configurations.

3. Because the various reactor configurations were obtained without substantial changes of the interzone coupling, Eq. (23) should define an invariant of the system. This result was substantiated by the experimental data, as shown in Table IV.

4. A comparison between the experimental and theoretical values of the A_i/B_i ratio is shown in Tables V and VI. The observed systematic differences can be explained as in item 1 by the fact that the model gives the behavior of global population and not the detailed space behavior. Nevertheless, the model correctly predicts the variations of the A_i/B_i ratio between different states.

5. The previous results show that the system is weakly coupled, hence, Eq. (37) can be used to

TABLE II

Comparison of $|\gamma_1|+|\gamma_2|$ and $|\alpha_1|+|\alpha_2|$ in Symmetrical Configurations for Different Rod Positions

Control Rod Position (% withdrawn)				sec^{-1}			
B_1	B_2	B_3	B_4	$\|\gamma_2\|$	$\|\gamma_1\|$	$\|\gamma_1\|+\|\gamma_2\|$	$\|\alpha_1\|+\|\alpha_2\|$
100	100	100	100	91.15 ± 0.70	892.2 ± 33.5	983.3 ± 34.2	963.1 ± 1.3
100	75	75	100	123.4 ± 0.5	899.0 ± 55.0	1022 ± 55	1039 ± 1
100	50	50	100	233.2 ± 1.3	1025 ± 103	1259 ± 104	1249 ± 1
100	25	25	100	365.6 ± 1.4	1137 ± 74	1503 ± 75	1507 ± 2
100	0	0	100	441.0 ± 2.6	1216 ± 45	1657 ± 48	1645 ± 2
0	100	100	0	592.1 ± 3.9	1423 ± 55	2015 ± 59	2044 ± 2
0	50	50	0	763.0 ± 18.0	1614 ± 89	2377 ± 107	2391 ± 3
0	0	0	0	1022 ± 22	1929 ± 168	2952 ± 190	2892 ± 4

TABLE III

Comparison of $|\gamma_1|+|\gamma_2|$ and $|\alpha_1|+|\alpha_2|$ in Asymmetrical Configuration for Different Rod Positions

Control Rod Position (% withdrawn)				sec^{-1}			
B_1	B_2	B_3	B_4	$\|\gamma_2\|$	$\|\gamma_1\|$	$\|\gamma_1\|+\|\gamma_2\|$	$\|\alpha_1\|+\|\alpha_2\|$
100	0	100	100	222.6 ± 4.7	1059 ± 59	1282 ± 64	1299 ± 2
100	0	100	0	318.4 ± 7.2	1455 ± 193	1733 ± 200	1907 ± 3
100	100	0	0	506.6 ± 6.5	1363 ± 54	1870 ± 61	1841 ± 2
0	0	0	100	640.8 ± 16.5	1601 ± 140	2242 ± 156	2284 ± 3
0	0	100	0	738.0 ± 13.0	1771 ± 121	2516 ± 134	2456 ± 4
0	100	100	100	256.4 ± 7.3	1240 ± 42	1496 ± 49	1512 ± 2

TABLE IV

The Function $\alpha_1\alpha_2 - \gamma_1\gamma_2$ as a Function of Rod Positions

Control Rod Position (% withdrawn)				$(10^3\ sec^{-2})$
B_1	B_2	B_3	B_4	$\alpha_1\alpha_2 - \gamma_1\gamma_2$
100	100	100	100	150.5 ± 3.2
100	75	75	100	158.9 ± 6.8
100	50	50	100	150.4 ± 24.1
100	25	25	100	151.6 ± 27.1
100	0	0	100	140.3 ± 20.1
0	100	100	0	201.3 ± 33.1
0	50	50	0	197.7 ± 74.2
0	0	0	0	116.2 ± 177.0
100	0	100	100	160.6 ± 14.1
100	0	100	0	230.2 ± 62.5
100	100	0	0	149.0 ± 29.0
0	0	0	100	168.1 ± 93.5
0	0	100	0	164.3 ± 92.6
0	100	100	100	174.1 ± 14.1

determine the reactivity. Table VI shows that the method based on Eq. (37) gives the correct results at criticality. For subcritical states, we verified the consistency of the method in the following manner. Equation (37) was utilized to calibrate the control rods. Then rod configurations, in which the shadowing effects were negligible, were also measured by the present method [Eq. (37)] and compared with the results expected from the additivity hypothesis. The results are shown in Table VII.

Table VIII shows the reactivity results obtained by the method based on Eq. (31). As expected, according to the restrictions associated with Eq. (31), the agreement is only good for small reactivities.

CONCLUSIONS

A model was developed to analyze the temporal behavior of a coupled reactor. Pulsed-neutron experiments in a weakly coupled two-core reactor were performed to test the model.

TABLE V

Comparison of Theoretical and Experimental Values of A/B in Region 1

Control Rod Position (% withdrawn)				$A/B = \frac{(\gamma_1 - \alpha_2)}{(\gamma_2 - \alpha_2)}$	A/B experimental
B_1	B_2	B_3	B_4		
100	75	75	100	0.90 ± 0.13	0.82 ± 0.03
100	50	50	100	0.95 ± 0.25	0.83 ± 0.02
100	25	25	100	0.92 ± 0.18	0.82 ± 0.02
100	0	0	100	0.97 ± 0.11	0.80 ± 0.05
0	100	100	0	0.86 ± 0.12	0.72 ± 0.08
0	50	50	0	0.85 ± 0.20	0.80 ± 0.09
0	0	0	0	0.93 ± 0.36	0.75 ± 0.05
100	0	100	100	2.14 ± 0.22	2.10 ± 0.07
100	0	100	0	5.66 ± 1.16	4.62 ± 2.12
100	100	0	0	1.61 ± 0.17	1.30 ± 0.07
0	0	0	100	0.21 ± 0.18	0.24 ± 0.02
0	100	100	100	0.18 ± 0.03	0.22 ± 0.01
0	0	100	0	2.44 ± 0.42	1.61 ± 0.25

TABLE VI

Comparison of Theoretical and Experimental Values of A/B in Region 2

Control Rod Position (% withdrawn)				A/B Theoretical	A/B Experimental
B_1	B_2	B_3	B_4		
100	75	75	100	-1	-0.68 ± 0.07
100	50	50	100	-1	-0.61 ± 0.10
100	25	25	100	-1	-0.79 ± 0.03
100	0	0	100	-1	-0.89 ± 0.07
0	100	100	0	-1	-0.83 ± 0.03
0	50	50	0	-1	-0.87 ± 0.08
0	0	0	0	-1	-0.92 ± 0.13
100	0	100	100	-1	-0.72 ± 0.09
100	0	100	0	-1	-0.83 ± 0.06
100	100	0	0	-1	-0.75 ± 0.11
0	0	0	100	-1	-0.94 ± 0.10
0	0	100	0	-1	-0.94 ± 0.05
0	100	100	100	-1	-0.71 ± 0.07

TABLE VII

Comparison of Reactivities Obtained by Calibration and Measured Directly, Both According to Eq. (37)

Control Rod Position (% withdrawn)				$ Calibration[a]	$ Directly[b]
B_1	B_2	B_3	B_4		
100	50	50	100	1.35 ± 0.24	1.31 ± 0.40
100	0	0	100	2.70 ± 0.48	2.94 ± 0.13
0	100	100	0	3.60 ± 0.34	4.20 ± 0.14
100	100	0	0	3.15 ± 0.41	3.50 ± 0.16

[a] The reactivity measurement of each control rod was made separately, and then the reactivity of the system was determined using the additivity hypothesis.

[b] The reactivity of the system was measured.

TABLE VIII

Reactivities in the Coupled Reactor According to Eq. (37) and Its Approximation, Eq. (31)

Control Rod Position (% withdrawn)				Reactivity from Eq. (37) (dollars)	Reactivity from Eq. (31) (dollars)
B_1	B_2	B_3	B_4		
100	100	100	100	0.07 ± 0.17	0.0
100	75	75	100	0.43 ± 0.24	0.36 ± 0.10
100	50	50	100	1.31 ± 0.40	1.94 ± 0.32
100	25	25	100	2.45 ± 0.24	4.11 ± 0.39
100	0	0	100	2.94 ± 0.13	5.59 ± 0.35
0	100	100	0	4.20 ± 0.14	9.40 ± 0.60
0	50	50	0	5.65 ± 0.21	14.10 ± 1.10
0	0	0	0	7.36 ± 0.34	23.2 ± 2.40
100	0	100	100	1.35 ± 0.24	1.90 ± 0.21
100	0	100	0	2.76 ± 0.71	4.70 ± 0.80
100	100	0	0	3.50 ± 0.16	7.50 ± 0.50
0	0	0	100	4.80 ± 0.37	11.6 ± 1.20
0	0	100	0	5.40 ± 0.33	15.1 ± 1.30
0	100	100	100	1.80 ± 0.17	2.90 ± 0.20

The experimental results confirm the following predictions of the model:

1. The time response of the system is accurately described with two exponentials.
2. The decay constants of the two components are indeed shown to be global-type parameters of the system.
3. The relations [Eqs. (22) and (23)] between the decay constants of the coupled reactor and the decay constants of the isolated cores were verified experimentally.
4. The relations between A_i/B_i ratios and the measured decay constants are verified on the average.

A global reactivity for the system was defined, and various measurements support the consistency of the method proposed to measured it, as well as its validity at critical.

In summary, the model studied in this work provides a good description of the global time behavior of the system, without giving detailed information on the space dependence of the flux within each region.

ACKNOWLEDGMENTS

We are grateful to the following persons from the Departamento de Reactores, Comisión Nacional de Energía Atómica, whose efforts made this work possible: A. Gomez, J. J. Piñeyro, and O. Rogulich.

Part of the equipment used in this work was granted by the International Atomic Energy Agency under Contract ARG/72/015.